Retention and flux characteristics of nanofiltration membranes during hemicellulose prehydrolysate concentration

Olumoye Ajao [a,*], Mohamed Rahni [b], Mariya Marinova [a], Hassan Chadjaa [b], Oumarou Savadogo [a]

[a] Research Unit on Energy Efficiency and Sustainable Development of the Forest Biorefinery, Chemical Engineering Department, Polytechnique Montreal, C.P. 6079 Succ. Centre-Ville, Montréal, QC H3C 3A7, Canada
[b] Centre National en Électrochimie et en Technologies Environnementales, 2263, avenue du Collège, Shawinigan, QC G9N 6V, Canada

HIGHLIGHTS

- Six organic membranes were screened for concentrating a Kraft hemicellulose prehydrolysate.
- The influence of the feed conditions on the retention properties and flux decline was evaluated.
- A response surface model was developed for optimizing the membrane filtration system.
- Nanofiltration membranes can be utilized in integrated biorefinery processes.

ARTICLE INFO

ABSTRACT

The prehydrolysate generated in the Kraft pulping process prior to cooking of wood chips can be converted into value added products such as furfural, ethanol or xylitol. To make a furfural biorefinery economically feasible, it is proposed to reduce the energy use and process equipment size by concentrating the prehydrolysate stream prior to conversion. This work demonstrates the feasibility of simultaneously concentrating the hemicellulosic sugars and acetic acid in the prehydrolysate solution from a Kraft dissolving pulp mill by nanofiltration membrane. The performances of 6 commercial organic membranes made of polyamide, cellulose acetate and polypiperazine amide polymers and of different Molecular Weights Cut Off (MWCO) were evaluated. Special attention was directed to high retention of sugars, acetic acid and furfural. A membrane with a MWCO of about 200 Da and total sugars retention of 99% was selected. Cleaning of the membrane using NaOH returned the permeate flux up to 75% of the pure water flux level prior to use. A response surface model correlating the permeate flux to the temperature and pressure of the system has been developed.

1. Introduction

Forest biomass comprises of three main types of polymers; cellulose, hemicellulose and lignin. In a Kraft dissolving pulp process, the hemicelluloses are typically extracted in a prehydrolysis step prior to chemical delignification of the wood chips. The prehydrolysate stream obtained is made up mainly of the hemicellulosic sugars (C_5 and C_6 sugars) along with lesser quantities of organic acids, phenolic compounds and furfural. The cellulose fibers are processed into pulp after delignification. The extracted hemicelluloses fraction is merged with the lignin fraction that is removed during delignification and usually directed to the recovery cycle where it is combusted to produce energy. A better use of the

hemicelluloses would be to divert the prehydrolysate stream and convert the sugars into biofuels or bioproducts such as ethanol, furfural or xylitol [1]. To minimize the cost of valorizing the sugars, concentration of the prehydrolysate is mandatory before the conversion of the sugars into any value added product. Concentration allows to reduce the energy consumption and the investment cost for the subsequent process steps of the biorefinery. The concentration objectives (component separation and final sugars concentration) depend on the targeted biorefinery final product. For a Kraft pulp mill that uses hardwood as a feedstock, it is proposed to produce furfural from the prehydrolysate through the dehydration of the C_5 sugars. The C_5 sugars in the prehydrolysate make up to 80% of the total sugars. Furfural is a platform chemical for bioproducts that can substitute industrial organic compounds, which are currently produced from fossil sources. Furfural can also be converted into liquid biofuels [1,2] or used as a solvent in
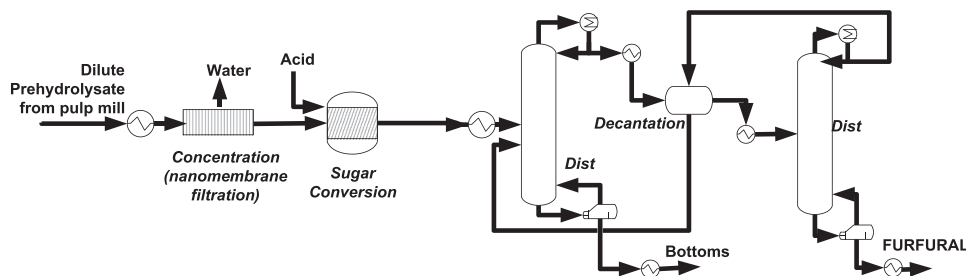
Fig. 1. Proposed biorefinery for producing furfural from hemicellulose prehydrolysate [5].
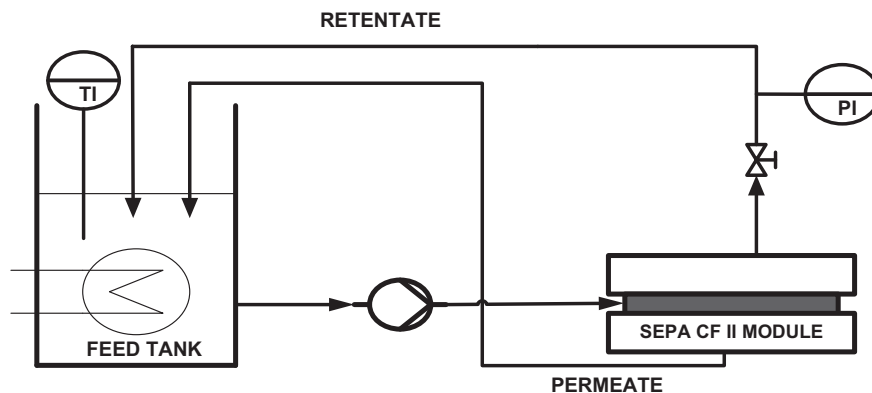

Fig. 2. Schematic membrane screening setup in closed loop mode.

petrochemical refineries [3] and as pesticides or nematocides [4]. A process for producing furfural from hemicelluloses prehydrolysate has been proposed by Ajao et al. [5] and it is illustrated in Fig. 1. After concentration of the prehydrolysate, the furfural is produced by two subsequent reactions; the oligomeric sugars in the prehydrolysate are hydrolyzed into sugar monomers which are then converted into furfural. A low pH is required to enhance the conversion process and this can be provided by introducing mineral acid into the reactor. Purification of furfural is done by distillation. Since furfural forms an azeotrope with water and has an azeotropic point of 35% wt, a decantation step is required between the two distillation columns to get above the azeotropic point.

In a biorefinery for furfural production, an important requirement for the concentration step is to retain the acetic acid along with the sugars; organic acids provide a low pH and act as catalysts, thereby reducing the mineral acid required for pentoses conversion to furfural [6]. Concentration with the typical use multi-effect evaporators is not feasible because the organic acids in the prehydrolysate are volatile and would be lost. Furthermore, evaporators have high energy consumption due to the latent heat for water that must be supplied. Membrane concentration on the other hand requires a lower amount of energy as it does not involve a phase change. The hemicellulose prehydrolysate treated in this work is a complex solution containing several organic compounds and the sugars present range from simple monomers to oligomers. The organic acids, phenolic compounds and furfural also influence the retention and flux that can be obtained during concentration [7]. The use of membrane filtration presents some challenges that must be addressed before economically feasible membrane concentration of prehydrolysate can be carried out. A suitable membrane that is capable of simultaneously retaining the sugars and organic acids with acceptable energy consumption must be used. Also, the occurrence of flux decline over the life of a membrane makes it important to determine if the operation would necessitate frequent cleaning or changing of the membrane. Lastly, there is a limit beyond which the permeate flux

of the membrane would be too low and further concentration of the prehydrolysate will not be possible. To the best of our knowledge, the application of membrane filtration to real prehydrolysate solution for a furfural biorefinery has not been investigated. Also, the effect of varied operating conditions on the flux decline has not been investigated. Thus, the objectives of this work have been to screen commercially available membrane suitable for hemicelluloses concentration, determine the flux reduction of a selected membrane over extended periods of use and develop a model relating the operating conditions to the membrane flux and useful life.

Screening of six commercial organic membranes made of polyamide, cellulose acetate and polypiperazine amide polymers and having different Molecular Cut Off Weights (MWCO) between 100 and 500 Da was carried out. In the screening experiments, the separation of components in a prehydrolysate solution generated from a wood supply similar to that of a Canadian dissolving pulp mill was determined for all membranes. The selected membrane for the concentration studies had a MWCO of about 200 Da. The effect of feed condition on flux decline has already been documented [7], this is the first paper to clearly demonstrate how it relates to the concentration of hemicelluloses prehydrolysate from a Kraft dissolving pulp process. The generated data could be applied to the design of efficient membrane concentration systems and successfully used in forest biorefinery processes.

2. Materials and methods

2.1. Prehydrolysate generation

The prehydrolysate used in this study was generated in a 56 L digester using a 60% Aspen–40% Maple wood furnish. The typical compositions of the wood chips are shown in Table 1.

The wood chips had a moisture content of 37% and were purged with steam (138 kPa) to remove the air content and preheat the

Table 1
Composition of maple and aspen wood chips (% by weight, dry basis).

Component	Maple wood (wt%)	Aspen wood (wt%)
Cellulose	44	50
Hemicellulose	23	23
Lignin	31	24
Extractives	2	3

Table 2
Composition of hemicellulose prehydrolysate generated for use in the experiments.

Components	Concentration (g/L)
Total sugars[*]	20.3
Total monomeric pentose	2.55
Total monomeric hexose	0.74
Acetic acid	3.8
Furfural	0.7
HMF	0.09
Phenolics	4.7
Lipides	0.2
Na	0.02
Ca	0.15
K	0.04

[*] Ratio of pentose to hexose is 4:1.

chips prior to cooking. After the digester had been sealed, prehydrolysis of the wood chips was carried out in two successive steps. In the first step, steam was introduced directly into the digester for 50 min until a pressure of 700 kPa and a temperature of 170 °C were reached, the temperature was held at this value for another 60 min. In the second step, deionized water at 80 °C was introduced into the digester and subsequently circulated through an external liquor heater to maintain the digester at 170 °C. The final prehydrolysate liquor to wood ratio was of 3:1. The key components of the prehydrolysate are given in Table 2. The pentoses (xylose and arabinose) and hexoses (glucose, galactose and mannose) are mainly in oligomeric form with only about 15% as monomers. The prehydrolysate had a total solid content of 3.4%. The pH and conductivity of the prehydrolysate solution were 3.52 and 1620 μS/cm, respectively.

2.2. Screened membranes

Six commercially available spiral wound organic membrane types were used in this study. They represent a broad range of material and Molecular Weight Cut Off (MWCO). The names and main characteristics of each membrane is given in Table 3. All membranes had similar pH operating range (2–11) and maximum temperature (45 °C).

Each membrane element was cut lengthwise and opened up. It was then soaked in a solution of 1% wt/vol of sodium metabisulfite to enable the pores to loosen up and prevent the growth of microorganisms. Prior to use, flat sheets were cut from the membrane

roll and placed in distilled water for at least 3 days to remove the sodium metabisulfite and condition them for use.

2.3. Membrane setup

The filtration experiments were carried out using a lab-scale cross-flow flat-sheet membrane test unit (SEPA CF II, GE Osmonics). It had a rectangular filtration channel with dimensions 14.5 cm × 9.6 cm × 1.0 mm for accommodating various kinds of flat-sheet membrane. The feed pressure to the unit was varied using a hydraulic hand pump (SPX maximum pressure 70,000 kPa).

The stainless steel feed tank had a capacity of 4 L and a hollow wall in which glycol was circulated to control the feed temperature. To screen the membranes in a continuous filtration mode, the permeate stream was directed back into the feed tank as shown in Fig. 2. Continuous filtration eliminates the effect of concentration on component separation during screening of the membranes. Concentration of the prehydrolysate was carried out in a batch mode during which the permeate stream is directed to a permeate cylinder.

2.4. Filtration procedure

Prior to concentration experiments, the six membranes were screened under similar conditions. A fresh membrane sheet was used for each experimental run. Prehydrolysate (1 L) was supplied into the feed tank and continuously filtered in a close loop run during the screening experimental runs, samples of about 10 mL were collected from the permeate and retentate streams over 90 min at 15 min intervals. The flow rate of the permeate stream was also measured at same intervals. During the concentration trials (batch mode), 2.5 L of prehydrolysate was introduced into the feed tank and a total of 2 L of permeate was withdrawn in a graduated cylinder to reach a volumetric concentration factor of 5. About 10 mL of permeate sample was taken after each 200 mL of withdrawn permeate. Samples of the retentate were taken from the feed tank before and after concentration. The amounts of sugars, organic acids, furfural and phenols in the collected samples were analyzed. In order to determine the degree of membrane fouling, the permeate volume flow (L/min) at specific pressures was measured before and after filtration of the prehydrolysate, using distilled water at a constant cross flow velocity of 0.4 m/s.

2.5. Analytical methods

Initial monomeric sugars concentration was measured using a Dionex DX600 ion chromatograph equipped with a pulsed amperometric detector and Carbopac PA1 column [8]. The total solubilized sugars were determined by hydrolyzing the sugars with 2.5% wt/vol of sulfuric acid for 20 min in an autoclave followed by sugar analysis. Organic acids were characterized by HPLC (Agilent Technologies, Germany) equipped with 210 nm diode array

Table 3
Characteristics of the reverse osmosis (RO) and nanofiltration (NF) membranes provided by suppliers.

	TW30	NF90	NF270	XN45	TS40	SB90
Manufacturer	Dow	Dow	Dow	Trisep	Trisep	Trisep
Polymer	Polyamide	Polyamide	Polyamide	Polypipera-zine amide	Polypipera-zine amide	Cellulose acetate blend
Max. pressure (kPa)	4100	4100	4100	4100[A]	4100[B]	4100[C]
Max. temperature (°C)	45	45	45	45	45	45
pH operating range	2–11	2–11	2–11	2–11	2–11	2–11
MWCO	~100	~200–400	~200–400	500	200	150
Nacl rejection (%)	99.5	>97	>97	10–30	40–60	85
Classification	RO	NF	NF	NF	NF	NF

[A–C] Recommended applied pressures (kPa), A: 275–1380; B: 275–1380; C: 1550.

detector (DAD) and an Inertsil ODS-3 (150 × 4.6 mm) column. The mobile phase was a mixture of 50 mM potassium phosphate that was adjusted to a pH of 2.8 with phosphoric acid (H_3PO_4) and acetonitrile (KH_2PO_4 99%–CH_3CN 1%) that was fed at 1.25 L/min into the column at 40 °C. Furfural and hydroxymethylfurfural were analyzed with the same HPLC but equipped with a 280 nm diode array detector (DAD) and a Nucleosil C18 column. The eluent used was a mixture of acetonitrile, water and acetic acid (CH_3CN 15%, H_2O 84% and $C_2H_4O_2$ 1%). The flow rate of the mobile phase was 1 mL/min and the column temperature was 25 °C. Phenols quantification was determined using Folin–Ciocalteu reagent colorimetric analysis, a method adapted from Singleton and Rossi [9]. After the membrane experimental runs, the dinitrosalicylic acid (DNS) colorimetric method [10] was used to determine the total reducing sugars in the feed, permeate and concentrate. The metal ions were quantified with an Optima 4300 DV Inductively coupled plasma atomic emission spectroscopy (PerkinElmer Inc., USA).

2.6. Experimental design and data analysis

Two design of experiments (DOE) methods were used in this study. The first was a $(2)^2$ factorial parametric study to determine the effect of pressure and cross flow velocity on separation characteristics of a selected membrane at a constant temperature. Response surface methodology (RSM), a DOE approach for developing a mathematical correlation between the operating conditions and observed responses of a process, was used to design the subsequent set of experiments. RSM can be applied to the development, improvement or optimization of processes. The main advantages of RSM are that it can be used to study the effect of multiple variables without neglecting the interaction effects using a small number of experiments [11]. Central composite design (CCD) and Box–Behnken design (BBD) are the two main RSM experiment designs [12]. RSM–BBD requires a lower number of experiments than CCD and was therefore selected for this study. Each measured response from the experiments (permeate flux and flux decline) was correlated with a second degree polynomial Eq. (1).

$$Y_i = b_0 + \sum_{i=1}^{n} b_i x_i + \sum_{i=1}^{n} b_{ii} x_i^2 + \sum_{i=1}^{n-1} \sum_{j=i+1}^{n} b_{ij} x_i x_j \tag{1}$$

In the equation, Y_i is the predicted response, b_0 the intercept term, b_i the linear coefficients, b_{ii} the 2nd order polynomial coefficient, b_{ij} the interaction term and x_i, x_j the coded values for the variables. In general a model with fewer terms which allows for good fit with the experimental data is selected while the terms that are not considered to be significant are neglected. STATISTICA 10 (StatSoft software, Inc.), was used for design of the experiments, data analysis and model building.

2.7. Measures of membrane performance

The volumetric concentration factor (CF) achieved during concentration with a given membrane cane defined in terms of the volume (V) of the prehydrolysate fed into the tank as given in Eq. (2).

$$CF = V_{initial}/V_{final} \tag{2}$$

In a closed loop run with no concentration such as the membrane screening experiments, $V_{initial} = V_{final}$ and the concentration factor is 1. The equivalent permeate flux J for the experimental runs, was estimated from a simplified relationship between the measured volume flow (Q) per unit membrane surface area (A) as shown in Eq. (3).

$$J = Q/A \tag{3}$$

To assess the separation performance of the membranes when subjected to different operating conditions (temperature, pressure and cross velocity), the percentage retention of the main organic compounds in the prehydrolysate were determined using Eq. (4).

$$\%R_i = \left(1 - \frac{C_{permeate}}{C_{feed}} \right)_i \times 100 \tag{4}$$

where $C_{permeate}$ represents the concentration of the ith component in the permeate stream and C_{feed}, the concentration in the feed solution. The recovery of the ith component can be calculated using mass balance relationship shown in Eq. (5).

$$C_{feed} V_{feed} = C_{permeate} V_{permeate} + C_{concentrate} V_{concentrate} \tag{5}$$

2.8. Membrane flux and flux decline mechanisms

A permeate flux decline occurs during concentration with a nanofiltration membrane. This can be attributed to increased osmotic pressure, fouling of the membrane, concentration polarization or compaction of the membrane. An increase in solute concentration results in an osmotic pressure increase. Consequently, it is necessary to supply a higher trans-membrane pressure to maintain the permeate flux as shown in Eq. (6), where ΔP is the trans-membrane pressure and $\Delta \pi$ the osmotic pressure difference between the feed and permeate side.

$$J_v = A_w(\Delta P - \Delta \pi) \tag{6}$$

A detailed overview of the mechanisms has been given in previously reported studies [13–15]. The ratio of the pure water flux observed with the membrane prior to concentration to the flux after prehydrolyte concentration was used as a measure of flux decline. The contribution of each of the prehydrolysate components to the flux decline mechanism has been shown in an earlier study [7]. The fouling tendency of a membrane is due to the combined effect of the pollutants in the solution, the membrane surface and pore characteristics and the operating conditions. Fouling is inevitable, although it can be reversible in some cases, it cannot be completely eliminated but only reduced [16]. A consequence of fouling is an increase of operation and maintenance (O&M) costs [17,18].

3. Results and discussion

3.1. Membrane screening

A comparison of the six membranes shown in Table 3 was carried out to determine the most suitable for concentrating the prehydrolysate solution. The criteria for selecting a suitable membrane were the energy requirement for concentration, fouling potential and the retention of desired components (sugars, acetic acid and furfural). Component retention is the most important criteria because it indicates which of the membranes should be used for recovering the sugars in the prehydrolysate. The energy requirement and fouling potential are secondary criteria for selecting between membranes with similar component retention. In addition, the fouling extent indicates the durability of the membranes.

3.1.1. Membrane power consumption

The power consumption of a nanofiltration membrane system can be attributed mainly to the high pressure pump. The power consumption (W) of the pump is a function of the feed flow rate (Q_f), feed pressure (P_f), and efficiency of the pump (η). The design feed pressure is a sum of the driving pressure, pressure on the permeate side, pressure drop in the system and osmotic pressure of

the solution. The pump efficiency comprises the electrical motor efficiency and the impeller efficiency.

$$W = \frac{Q_f P_f}{\eta} \qquad (7)$$

The operating pressure versus permeate flow curves were plotted for each of the membranes as shown in Fig. 3. An equivalent pure water permeate flow rate (30 mL/min), that lies within the operating pressure range for all the membranes, was used to determine the operating pressures for the screening experiments.

The permeate flow for the Trisep SB90 and Dow TW30 membranes overlap. Their power requirement is proportional to the operating pressure and lowest for the XN45 membrane. The determined order of their power requirements are TW30~SB90 > TS40 > NF270 > NF90 > XN45. Although the membrane polymers have different structure, this trend could be explained by the looseness of the membranes, which is indicated by their Molecular Weight Cut Off (MWCO). The determined pressure corresponding to a permeate flow rate of 30 mL/min was used for the filtration runs to determine component retention.

3.1.2. Component retention

The second screening criterion was the component retention. Closed loop filtration runs to determine the retentions of the main prehydrolysate components (sugars, acetic acid, furfural and phenols) were carried out at the predetermined equivalent pressures for each membrane to enable comparison at the same permeate flow rate. Analysis of the permeate and concentrate streams gave the percentage retentions of each component and the results are given in Fig. 4.

High sugar retentions were exhibited by the TW30 (99%), NF90 (99%), SB90 (98%) and TS40 (97%) membranes, respectively. In addition, the TW30 and the NF90 also produced the highest acetic acid and furfural retentions. A high retention of acetic acid is important because it produces a low pH that catalyzes sugar conversion into furfural. A membrane with high furfural retention will

increase the recovery of furfural present in the prehydrolysate. The retention exhibited by a membrane is due to the interaction between three set of factors [19]: (1) The membrane characteristics (Molecular Weight Cut Off. electrostatic charge and hydrophobicity); (2) the characteristics of the prehydrolysate solution (size, electrostatic charge, geometry and hydrophobicity of the solute molecules as well as the ionic strength and pH of the solution); (3) the operating conditions and parameters (cross flow velocity, transmembrane pressure, flow channel configuration). However, the mechanisms that govern the retention of the organic compounds are complex and limited knowledge is available [20]. Therefore, data on retention for organic compounds are derived mainly from experimental observation in industrial process applications [21]. Experimental observation is also required for the prehydrolysate solution because it comprises of several organic compounds with different characteristics.

3.1.3. Flux decline

The feasibility of membrane filtration application depends on the ability to operate the system over long periods at acceptable permeate flux levels. However, a permeate flux decline was always observed. It is caused by compaction of the membrane under pressure, membrane fouling (deposition of organic or inorganic materials on the membrane surface) or increased osmotic pressure of the feed solution. The flux reduction observed after continuous operation of the membrane system over 6 h were classified as either physically reversible or chemically reversible for each membrane as shown in Fig. 5. Physically reversible flux decline refers to the relative pure water permeate flux before use to the flux after it has been used for concentration and subsequently cleaned with distilled water only. Chemical reversible decline is the relative pure water permeate flux after use and subsequent cleaning with a NaOH solution at a pH of 11.

It was observed that the relative flux after chemical cleaning was lower for the polyamide membranes (TW30, NF90 and NF 270) than for the cellulose acetate (SB90) and polypiperazine
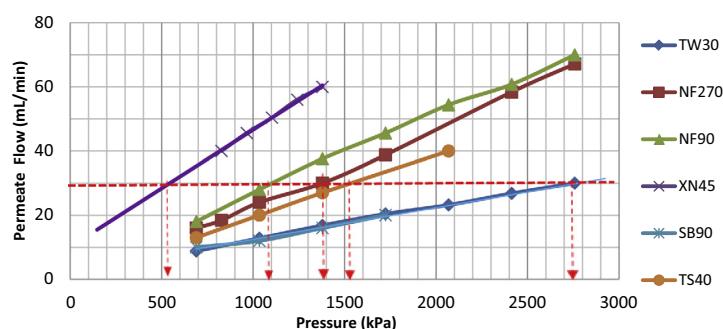

Fig. 3. Pure water permeate flux and equivalent pressures for component retention screening.
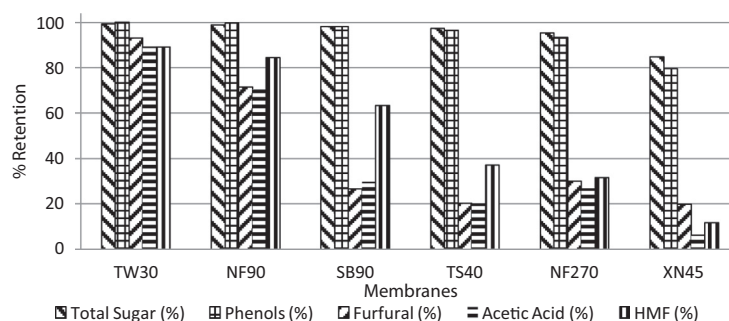

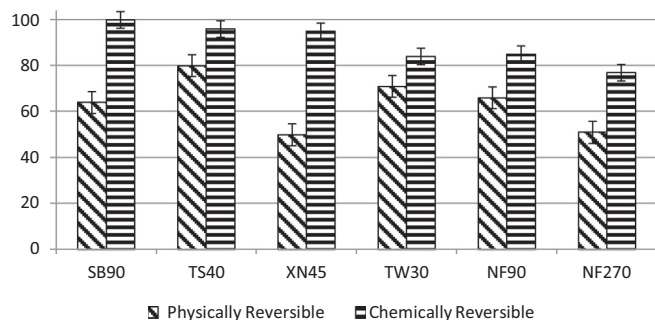**Fig. 4.** Retentions of the main components by each membrane from highest to lowest.

Fig. 5. Relative pure water flux after concentration followed physical and chemical cleaning of membranes (indexed to virgin membrane).

amide (TS40 and XN45) membranes. It is therefore important to determine if the irreversibility is due to fouling, compaction of the membrane for a membrane to be used for concentration. The results, which show that compaction can explain this observation, is discussed in Section 3.2.

3.2. Membrane selection

On the basis of total sugars rejection, only the XN45 membrane was eliminated because its component retention was inferior to 95%. The highest acetic acid and furfural retention were observed for the TW30 and NF90 membranes respectively, both membranes also exhibited a similar degree of fouling. The NF90 is more suitable for concentration from an energy standpoint because the sugar retention is comparable to that of the TW30 but the power requirement is only about 1/3 that of the TW30 membrane. The NF90 membrane was judged to be the most suitable membrane based on the results from the three screening criteria (component retention, flux decline and power consumption). To determine whether the flux decline exhibited by the NF90 despite chemical cleaning can be attributed to compaction of the membrane, confirmatory tests were carried out. The tests required continuous operation of the membrane filtration over a period of 4.5 h. Distilled water was filtered to ensure that the effect of the other flux decline mechanisms (fouling, concentration polarization and osmotic pressure increase) were eliminated while the feed conditions were similar to that of the prehydrolysate screening runs. It was observed that the flux recovery in all cases were in the same range as shown in Fig. 5. Hence, it can be concluded that compaction plays an

important role in the flux decline after membrane use but the decline can be compensated for by using a larger membrane surface area during the design phase of the membrane concentration system.

3.3. Prehydrolysate concentration

The selected membrane (NF90) was used in all the subsequent experiments. The experimental design shown in Table 4 was used to investigate the effect of varied operating pressure and cross velocities at a constant temperature on the component retention and permeate flux decline.

The observed components retention are shown in Fig. 6. The sugars retention was 99% in all 4 experiments. The total phenolics retention also exhibited the same tendency in all 4 experiments.

On the other hand, the furfural and acetic acid retentions were similar for all experiments except experiment #1, where they were slightly higher. This could be due to the high cross velocity at the low pressure range of the experiments. The observed permeate flux trend for the 4 test conditions are shown in Fig. 7. Although the initial permeate flow in experiment #2 was is higher than for the other experiments (10 versus ∼6 mL/min), they all tend to converge at a concentration factor of 5. The total duration of the concentration runs were #1 (8 h), #2 (7 h), #3 (10 h) and #4 (12 h). The experiments at a high cross velocity (#1 and #2) required a shorter time to reach a concentration factor of 5. The viscosity increase of the feed is more pronounced at a concentration factor of 5. Hence, only concentrating to a factor of about 4 can be useful in reducing the fouling of the membrane. Furthermore, the observed equivalent permeate flux of about 12 L/m^{2}h at this concentration factor, can be considered acceptable for a pilot scale system.

The results confirm that it is technically feasible to concentrate the prehydrolysate solution up to a volumetric concentration factor (VCF) of 5. Sugars retention of 99% can be achieved while average

Table 4
Test conditions to determine the influence of operating conditions on component separation.

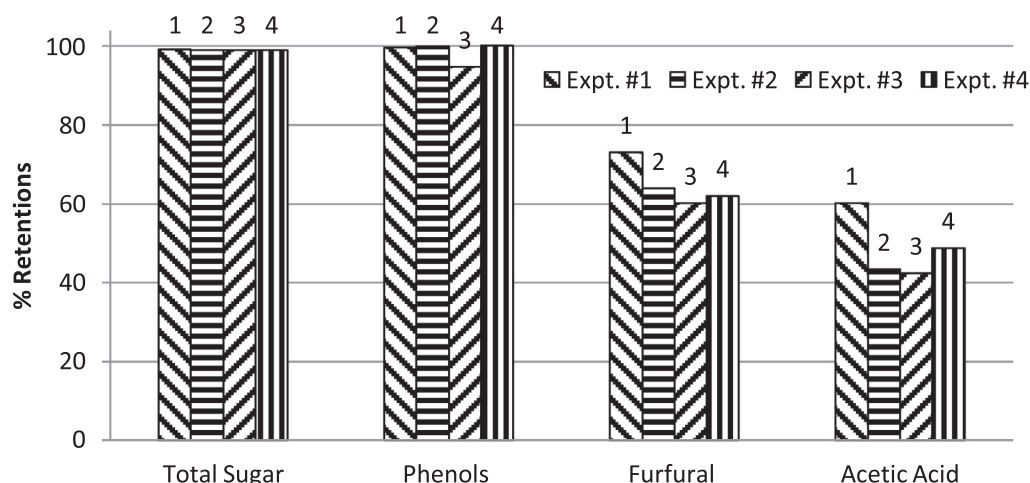| Expt.	Pres. (kPa)	Cross vel. (m/s)	Temp. (°C)
1	2100	0.66	40
2	3500	0.66	40
3	2100	0.45	40
4	3500	0.45	40

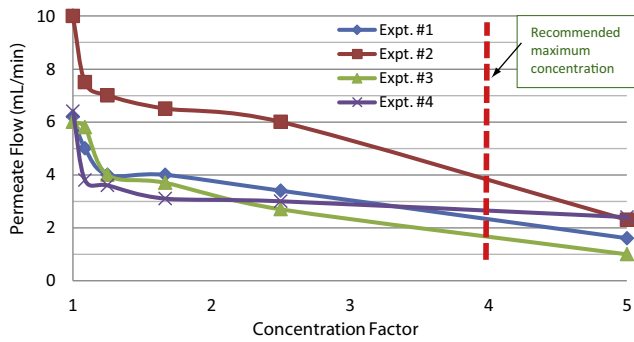**Fig. 6.** Comparison of component retentions for the four experiments (%).

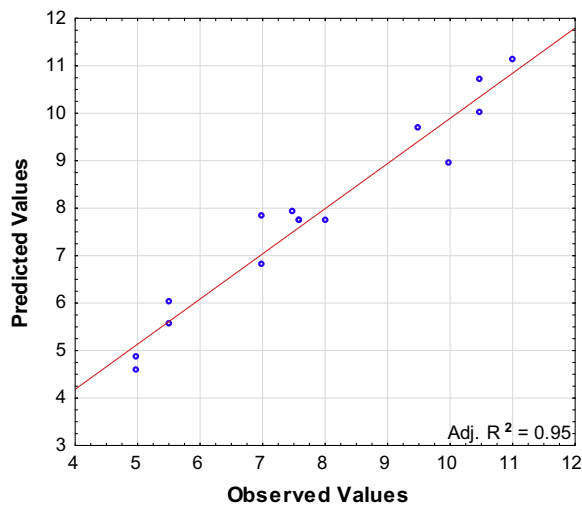Fig. 7. Permeate fluxes as a function of concentration factor for Exp. 1–4.

Fig. 8. Observed initial permeate flux versus the values predicted by Eq. (8).

acetic acid retention of 50% was observed. In all cases the pH of the prehydrolysate dropped from 3.7 to about 2.9 after concentration, this is in the range expected for acetic acid retentions approaching 100%. Hemicellulosic sugars concentration is technically feasible but the economic feasibility will depend on the possibility to obtain a sufficiently high permeate flux and to minimize the flux decline during prehydrolysate concentration. A permeate flow that is higher than 3 mL/min (12 L/m^{2}h) would be suitable at an industrial scale. The frequency of cleaning for an industrial membrane system could range between 7 and 180 days depending on the degree of fouling while the life of the membrane element could be between 1 and 5 years. A low flux decline will prevent the need for frequent cleaning and replacement of the membrane elements.

3.4. Response surface optimization of membrane life and operating conditions

To determine the most suitable operating conditions for prehydrolysate concentration, it is necessary establish the relationships between the initial permeate flux and the operating conditions, and the operating conditions that would result in a low flux decline. This was achieved using the response surface model Box–Behnken experimental design (RSM-BBD) described in Section 2.6. The RSM-BBD consisted of 15 experiments with 3 levels for pressure, cross velocity and temperature with their coded values shown in Table 5. The coding notations are: −1 (minimum), 0 (central) and 1 (maximum).

Table 5
Coded variables levels for the Box–Behnken design (BBD).

Controlling factors	Coded levels			Units
	−1	0	1	
X_1 (pressure)	1050	1500	2050	kPa
X_2 (cross velocity)	0.45	0.56	0.66	m/s
X_3 (temperature)	22	30	40	C

Table 6
RSM–BBD design matrix and experimental results.

Exp. No.	Input variables			Response	
	X_1	X_2	X_3	Y_1	Y_2
1	1	0	−1	9.5	1.9
2	0	1	1	10.0	2.8
3	1	−1	0	10.5	2.1
4	0	0	0	8.0	2.1
5	−1	0	−1	5.0	1.9
6	0	0	0	7.6	2.0
7	1	0	1	10.5	2.4
8	0	−1	1	7.0	2.3
9	0	−1	−1	7.0	1.9
10	0	1	−1	7.5	1.9
11	0	0	0	7.6	2.1
12	−1	1	0	5.5	1.8
13	−1	0	1	5.5	2.5
14	−1	−1	0	5.0	2.1
15	1	1	0	11.0	1.9

Y_1: initial permeate flow.
Y_2: initial permeate flow/final permeate flow.

The design matrix and the measured results for the 15 experimental runs are shown in Table 6.

3.4.1. Permeate flux

Analysis of Variance (ANOVA) was used to determine the significance of the parameters (linear or quadratic) and the corresponding interaction terms to be used for fitting the response surface model in Eq. (8). The ANOVA results table shown in Table 7 consists of several statistical terms: the sum of squares (SS), the variance (MS), degree of freedom (DF), F-ratio and p-value (p). The F-ratio (F) is the ratio of the variance by each parameter to the residual variance (error). It gives the magnitude of the effect of each parameter. The p value is the test for significance that shows the probability of obtaining the calculated values of F-ratio. The p value is considered significant for any term when $p < 0.05$ and it is to be

Table 7
ANOVA table for the model of initial permeate flux.

	Coeff.	SS	DF	MS	F	p	Remarks
X_1	5.14	52.39	1	52.4	221.4	2E−05	Significant
X_1^2	0.16	0.10	1	0.1	0.4	0.55	Insignificant
X_2	1.20	2.83	1	2.8	12.0	0.02	Significant
X_2^2	−0.29	0.30	1	0.3	1.3	0.31	Insignificant
X_3	0.98	1.90	1	1.9	8.0	0.04	Significant
X_3^2	0.17	0.11	1	0.1	0.5	0.53	Insignificant
$X_1 * X_2$	−0.05	3E−03	1	3E−03	1E−02	0.91	Insignificant
$X_1 * X_3$	0.19	0.04	1	4E−02	0.2	0.71	Insignificant
$X_2 * X_3$	1.30	1.70	1	1.7	7.2	0.04	Significant
Intercept	7.90					3E−08	Significant
Residue		1.18	5	0.2			
Total SS		60.30	14				

$R^2 = 0.98$, adjusted $R^2 = 0.95$

SS, sum of squares; DF, degree of freedom; MS, mean sum of square.
F, F-value; p, p-value and coeff., coefficient estimates.

included in the response model while it is considered as marginally significant for $p < 0.1$ and could still be included in the response model depending on the fit. R^2 indicates the fraction of the variance that can be accounted for by the model; a high R^2 value indicates a good fit between the model and the data [22]. A modified version of the R^2 to compensate for the number of predictors in the model is known as the Adjusted R^2.

Based on the results, it was found that the relationship between the initial permeate flux and the three input parameters, feed pressure (X_1), cross velocity (X_2) and temperature (X_3) in terms of the coded values can be fitted to a simple first order Eq. (8):

$$Y_1 = 7.90 + 5.14X_1 + 1.20X_2 + 0.97X_3 + 1.30X_2 * X_3 \qquad (8)$$

The corresponding significant coefficient estimates for the equation are as shown in Table 7. The predicted values of initial permeate flux were compared to the experimental value from Eq. (8) and showed to be in agreement (Fig. 8).

The retained terms in the equation suggests that the pressure followed by the cross velocity and temperature have a linear effect on the initial flux. This is confirmed in Fig. 9, that shows the change in permeate flux corresponding to the pressure, cross velocity and temperature. Fig. 9A illustrates the interaction between the cross velocity and pressure at a temperature of 30 °C. As expected, the pressure has the dominant effect on the initial permeate flow because the permeate flux is pressure driven. The same trend is
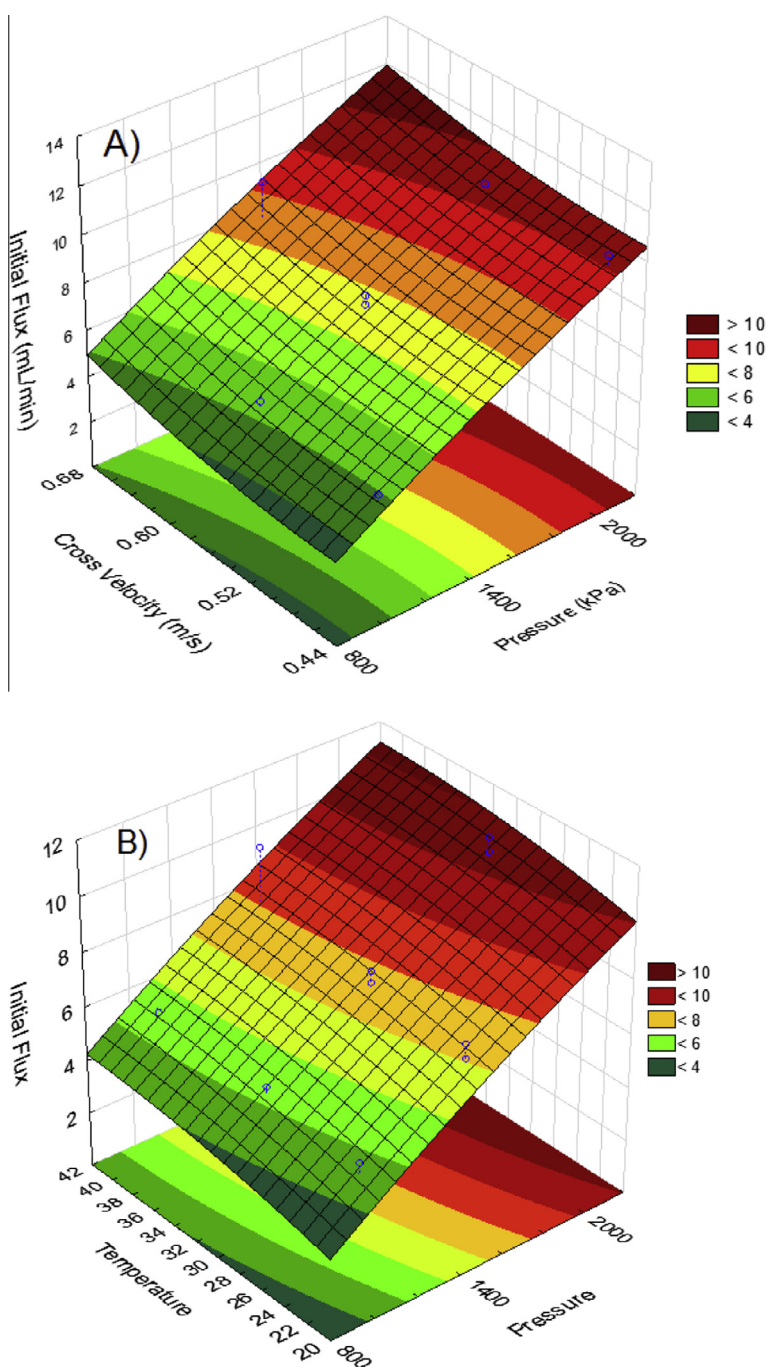

Fig. 9. Response surface of the combined effects of (A) cross velocity and pressure (B) feed temperature and pressure on initial permeate flow.
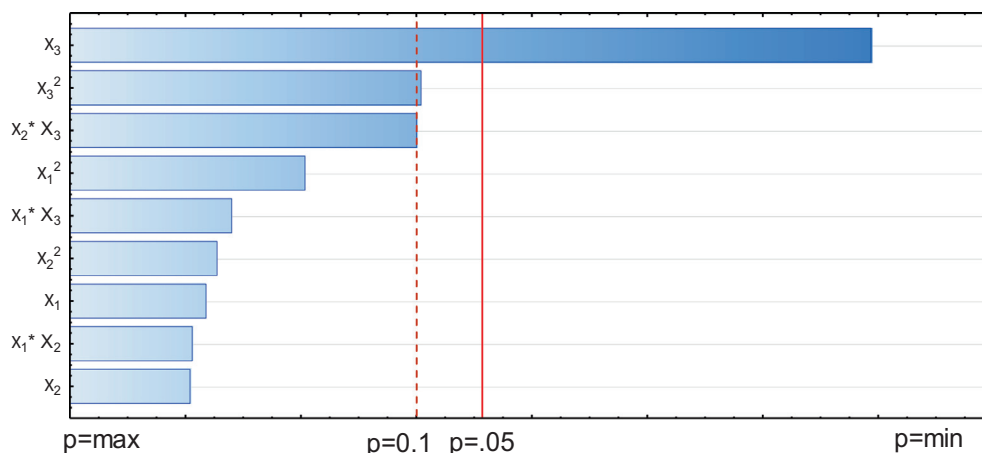
Fig. 10. Pareto chart of standardized effects for permeate flux decline.

shown in Fig. 9B, in which the effect of the feed pressure is superior to that of the temperature.

The significance of the pressure effect shows that it is important to start concentration at feed pressures less than 1050 kPa so that the flux decline can be compensated by increasing the pressure.

3.4.2. Permeate flux decline during concentration

Given that the prehydrolysate from a Kraft dissolving pulp mill will be available to a furfural biorefinery at a temperature of 80 °C or higher, it must be cooled down prior to concentration because the maximum temperature that can be tolerated by the organic membranes is 45 °C. Although it must be cooled to less than 45 °C, the cooling must be minimized because the prehydrolysate must be again reheated after concentration to a temperature of about 200 °C for the conversion of the pentose sugars into furfural. In addition, it was also observed during handling that prehydrolysate cooling resulted in increased precipitation that became pronounced at temperatures lower than 20 °C. The response surface model could be used in this case to determine the maximum tolerable prehydrolysate temperature that will minimize the decline of permeate flux during concentration. Analysis of Variance (ANOVA) was also used to determine the fitness of the model, the parameters (linear or quadratic) from Eq. (1) and their corresponding interaction terms to be used for fitting the response surface model in Eq. (9). The ANOVA results are illustrated in Fig. 10. The Pareto chart shows magnitude and the importance of the effect each term that can be included in the response surface model. Only the first three terms with acceptable p-values ($p \leqslant 0.1$) were included in the response surface model. They were the temperature linear term (X_3), temperature quadratic term (X_3^2) and the interaction between the temperature and cross velocity ($X_2 * X_3$).

The temperature has the highest impact on the flux decline and thus the useful life of the membrane within the range of feed conditions considered for the prehydrolysate. It was found that the relationship between the initial permeate flux and the three input parameters, feed pressure (X_1), cross velocity (X_2) and temperature (X_3) could be fitted to the second order polynomial Eq. (9):

$$Y_2 = 2.14 + 0.58X_3 - 0.147X_3^2 + 0.275X_2 * X_3 \tag{9}$$

The response model had an R^2 value of 0.91 and an adjusted R^2 of 0.74 (see Fig. 11). The adjusted R^2 value was considered a sufficient measure of fit because there are other factors related to the prehydrolysate that could also contribute to flux decline, such as increased osmotic pressure, fouling and concentration polarization.

The response surfaces in Fig. 12 showing the flux decline variation with the feed temperature, pressure and cross velocity is based on Eq. (9). The nonlinear effect of pressure on the flux decline is seen in the contour lines in Fig. 12A while a linear effect is observed for cross velocity in Fig. 12B. Obviously, Fig. 12A and B show that the temperature plays the dominant role in the flux decline. It can also be seen that the flux decline at a temperature of 32 °C is only about 10% higher than the flux decline at 20 °C. The maximum recommended temperature for limiting the flux decline due to the operating conditions in both response surfaces are in agreement. The effect of temperature was confirmed by two pure water filtrations tests conducted at a cross velocity of 0.45 m/s and a feed pressure of 3450 kPa. The feed temperature was kept at 22 °C during the first test and at 40 °C for the second test. It was observed that despite the high feed pressure applied over 4.5 h, the flux decline was less than 12% for the filtration run at 22 °C whereas it was as high as 36% when the temperature was raised to 40 °C. It can thus be concluded that high temperature could result in flux decline through irreversible membrane compaction. The effect of temperature could be further compounded when the membrane is subjected to high pressure.

The selected nanofiltration membrane (NF90) produced high sugars retention (99%) and a suitable permeate flux (12 L/m²h) during the concentration of the prehydrolysate solution by a factor of 5. The total sugars concentrations increased from 21 to 103 g/L.
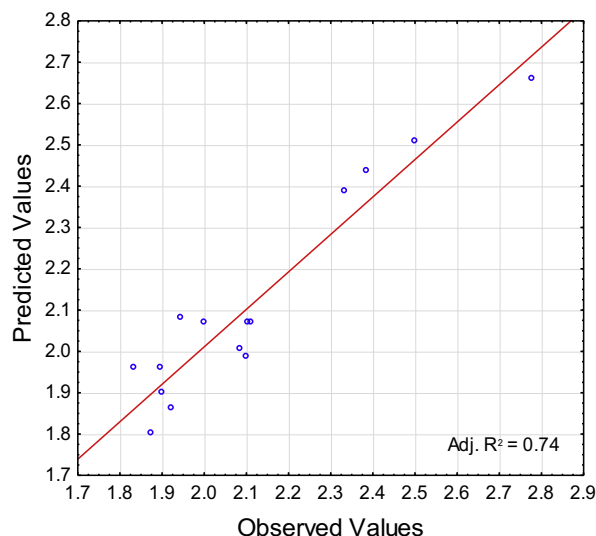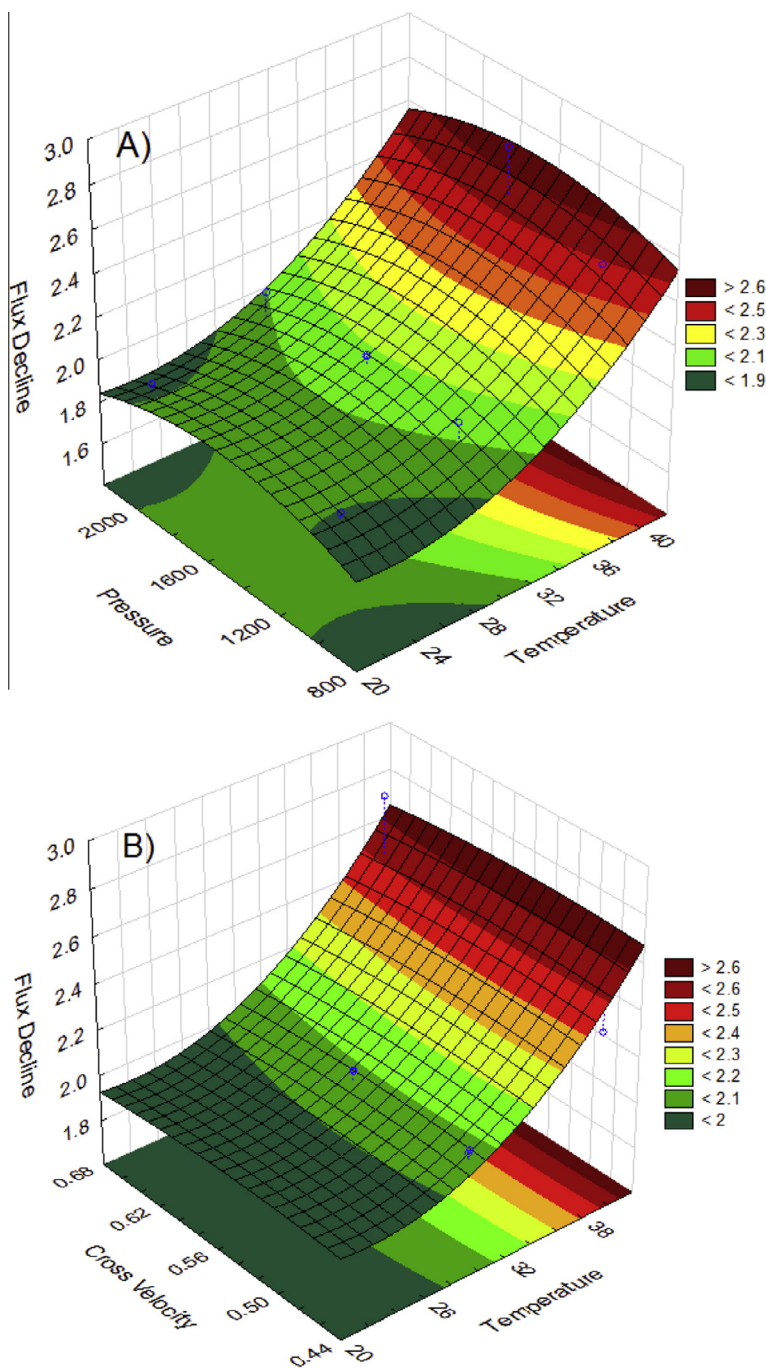

Fig. 11. Observed initial permeate flux versus the values predicted by Eq. (9).

Fig. 12. Response surface of flux decline, the combined effects of (A) feed pressure and temperature (B) cross velocity and temperature.

Operating the membrane system at a pressure inferior to 1050 kPa allows for compensation of flux reduction during concentration.

4. Conclusion

Six organic membranes that differ in MWCO and polymer material were evaluated for their ability to concentrate hemicellulosic sugars, organic acids and furfural in a prehydrolysate solution from a Kraft dissolving pulp mill. The experiments have shown that nanofiltration can be applied to a wide range of hemicellulose prehydrolysate solutions in the forest biorefinery context. The membrane selection results can provide data for similar biorefinery processes involving a chemical conversion of the sugars. Results

from this study also clearly demonstrate that RSM is an effective method for optimizing membrane filtration systems. It was used to determine the feed conditions that will lead to a long membrane life and at the same time reduce the energy required to reheat the prehydrolysate after concentration. Future research should include pilot scale experiments to enable a detailed economic analysis of the membrane system in a biorefinery process.

References

[1] J.-P. Lange, E. van der Heide, J. van Buijtenen, R. Price, Furfural—a promising platform for lignocellulosic biofuels, ChemSusChem 5 (2012) 150–166.

[2] S. Dutta, S. De, B. Saha, M.I. Alam, Advances in conversion of hemicellulosic biomass to furfural and upgrading to biofuels, Catal. Sci. Technol. 2 (2012) 2025–2036.

[3] L.P. Christopher, Integrated forest biorefineries: current state and development potential, Integrated forest biorefineries: challenges and opportunities, R. Soc. Chem. (2012) 1–66, http://dx.doi.org/10.1039/9781849735063-00001.

[4] J.A. Johnson, S.S. Walse, J.S. Gerik, Status of alternatives for methyl bromide in the United States, Outlooks Pest Manag. 23 (2012) 53–58.

[5] O. Ajao, M. Rahni, H. Chadjaa, M. Marinova, O. Savadogo, J. Paris, Hemicelluloses concentration and recovery using reverse osmosis (RO) membrane: application to an integrated biorefinery for furfural production, in: 63rd Canadian Chemical Engineering Conference, Fredericton, New Brunswick, 2013.

[6] K. Lamminpää, J. Ahola, J. Tanskanen, Kinetics of xylose dehydration into furfural in formic acid, Ind. Eng. Chem. Res. 51 (2012) 6297–6303.

[7] O. Ajao, M. Rahni, M. Marinova, H. Chadjaa, O. Savadogo, Concentration of hemicelluloses prehydrolysate by membrane filtration: feasibility and effect of composition on flux decline mechanisms, Sep. Purif. Technol. (2014) (Submitted).

[8] T. Radiotis, X. Zhang, M. Paice, V. Byrne, Optimizing hardwood prehydrolysis for simultaneous production of bioproducts and biomaterials, J. Bioprocess Eng. Biorefinery 1 (2012) 69–76.

[9] V.L. Singleton, J.A. Rossi, Colorimetry of total phenolics with phosphomolybdic–phosphotungstic acid reagents, Am. J. Enol. Viticult. 16 (1965) 144–158.

[10] I.P. Wood, A. Elliston, P. Ryden, I. Bancroft, I.N. Roberts, K.W. Waldron, Rapid quantification of reducing sugars in biomass hydrolysates: improving the speed and precision of the dinitrosalicylic acid assay, Biomass Bioenergy 44 (2012) 117–121.

[11] Y. Mo, L. Zhao, Z. Wang, C.-L. Chen, G.-Y.A. Tan, J.-Y. Wang, Enhanced styrene recovery from waste polystyrene pyrolysis using response surface methodology coupled with Box–Behnken design, Waste Manage. 34 (2014) 763–769.

[12] M. Tian, H. Park, K.H. Row, Optimization of synthesis amounts of polymers with two monomers by different methods based on response surface methodology, Adv. Polym. Technol. 33 (2014) (n/a–n/a).

[13] S. Stade, M. Kallioinen, A. Mikkola, T. Tuuva, M. Mänttäri, Reversible and irreversible compaction of ultrafiltration membranes, Sep. Purif. Technol. 118 (2013) 127–134.

[14] K.M. Persson, V. Gekas, G. Trägårdh, Study of membrane compaction and its influence on ultrafiltration water permeability, J. Membr. Sci. 100 (1995) 155–162.

[15] S. Déon, P. Dutournié, P. Fievet, L. Limousy, P. Bourseau, Concentration polarization phenomenon during the nanofiltration of multi-ionic solutions: influence of the filtrated solution and operating conditions, Water Res. 47 (2013) 2260–2272.

[16] J.I. Marriott, Detailed modelling and optimal design of membrane separation systems, in: University of London, 2001.

[17] Q. Zhang, C.D. Vecitis, Conductive CNT-PVDF membrane for capacitive organic fouling reduction, J. Membr. Sci. 459 (2014) 143–156.

[18] M.T.M. Pendergast, J.M. Nygaard, A.K. Ghosh, E.M.V. Hoek, Using nanocomposite materials technology to understand and control reverse osmosis membrane compaction, Desalination 261 (2010) 255–263.

[19] Y.-L. Lin, C.-H. Lee, Elucidating the rejection mechanisms of PPCPs by nanofiltration and reverse osmosis membranes, Ind. Eng. Chem. Res. 53 (2014) 6798–6806.

[20] A. De Munari, A.J.C. Semiao, B. Antizar-Ladislao, Retention of pesticide Endosulfan by nanofiltration: influence of organic matter–pesticide complexation and solute–membrane interactions, Water Res. 47 (2013) 3484–3496.

[21] C. Bellona, J.E. Drewes, P. Xu, G. Amy, Factors affecting the rejection of organic solutes during NF/RO treatment—a literature review, Water Res. 38 (2004) 2795–2809.

[22] P. Qiu, M. Cui, K. Kang, B. Park, Y. Son, E. Khim, M. Jang, J. Khim, Application of Box–Behnken design with response surface methodology for modeling and optimizing ultrasonic oxidation of arsenite with H_2O_2, Cent. Eur. J. Chem. 12 (2014) 164–172.